

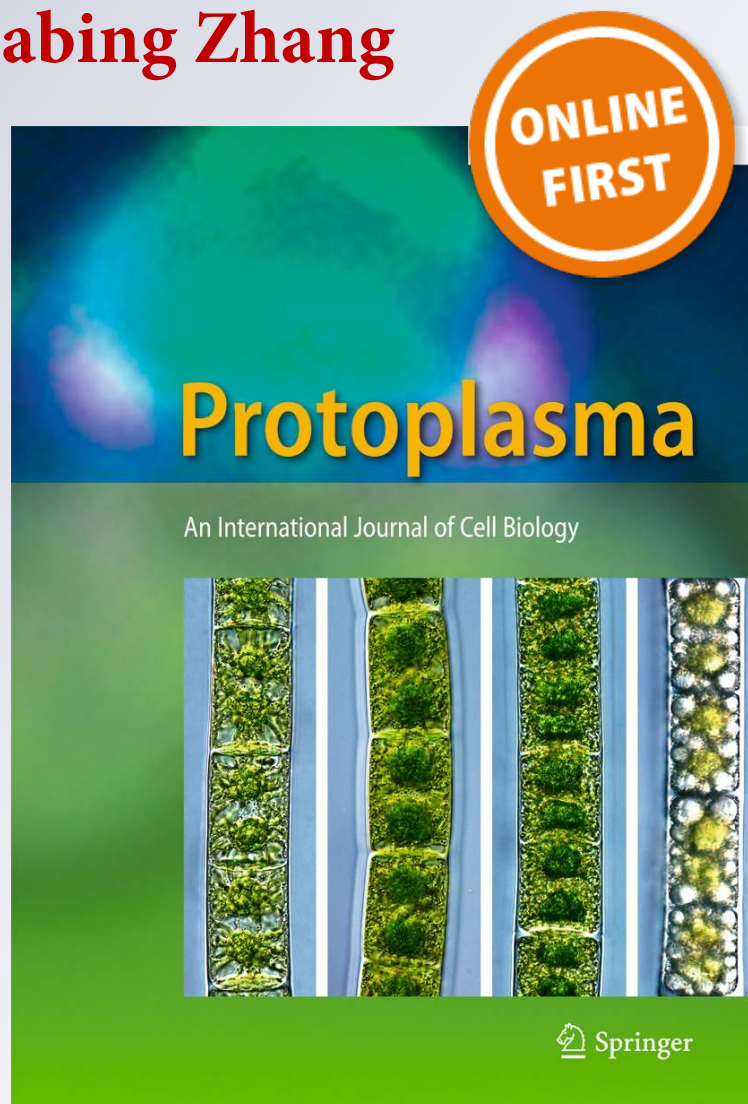
# *Cytological characterization of anther development in Panax ginseng Meyer*

**Yu-Jin Kim, Moon-Gi Jang, Lu Zhu,  
Jeniffer Silva, Xiaolei Zhu, Johan  
Sukweenadhi, Woo-Saeng Kwon, Deok-  
Chun Yang & Dabing Zhang**

**Protoplasma**  
An International Journal of Cell Biology

ISSN 0033-183X

Protoplasma  
DOI 10.1007/s00709-015-0869-3



**Your article is protected by copyright and all rights are held exclusively by Springer-Verlag Wien. This e-offprint is for personal use only and shall not be self-archived in electronic repositories. If you wish to self-archive your article, please use the accepted manuscript version for posting on your own website. You may further deposit the accepted manuscript version in any repository, provided it is only made publicly available 12 months after official publication or later and provided acknowledgement is given to the original source of publication and a link is inserted to the published article on Springer's website. The link must be accompanied by the following text: "The final publication is available at [link.springer.com](http://link.springer.com)".**

# Cytological characterization of anther development in *Panax ginseng* Meyer

Yu-Jin Kim<sup>1,2</sup> · Moon-Gi Jang<sup>1</sup> · Lu Zhu<sup>2</sup> · Jeniffer Silva<sup>1</sup> · Xiaolei Zhu<sup>2</sup> ·  
Johan Sukweenadhi<sup>1</sup> · Woo-Saeng Kwon<sup>1</sup> · Deok-Chun Yang<sup>1</sup> · Dabing Zhang<sup>2,3,4</sup>

Received: 15 March 2015 / Accepted: 5 August 2015  
© Springer-Verlag Wien 2015

**Abstract** Ginseng (*Panax ginseng*), a valued medicinal herb, is a slow-growing plant that flowers after 3 years of growth with the formation of a solitary terminal umbel inflorescence. However, little is known about cytological events during ginseng reproduction, such as the development of the male organ, the stamen. To better understand the mechanism controlling ginseng male reproductive development, here, we investigated the inflorescence and flower structure of ginseng. Moreover, we performed cytological analysis of anther morphogenesis and showed the common and specialized cytolog-

ical events including the formation of four concentric cell layers surrounding male reproductive cells followed by subsequent cell differentiation and degeneration of tapetal cells, as well as the formation of mature pollen grains via meiosis and mitosis during ginseng anther development. Particularly, our transverse section and microscopic observations showed that the ginseng tapetal layer exhibits obvious nonsynchronous cell division evidenced by the observation of one or two tapetal layers frequently observed in one anther lobe, suggesting the unique control of cell division. To facilitate the future study on ginseng male reproduction, we grouped the anther development into 10 developmental stages according to the characterized cytological events.

Handling Editor: Benedikt Kost

Yu-Jin Kim, Moon-Gi Jang and Lu Zhu contributed equally to this work.

**Electronic supplementary material** The online version of this article (doi:10.1007/s00709-015-0869-3) contains supplementary material, which is available to authorized users.

✉ Yu-Jin Kim  
yujinkim@khu.ac.kr

✉ Deok-Chun Yang  
dcyang@khu.ac.kr

<sup>1</sup> Department of Oriental Medicine Biotechnology and Graduate School of Biotechnology, College of Life Science, Kyung Hee University, Youngin 446-701, South Korea

<sup>2</sup> Joint International Research Laboratory of Metabolic and Developmental Sciences, Shanghai Jiao Tong University–University of Adelaide Joint Centre for Agriculture and Health, School of Life Sciences and Biotechnology, Shanghai Jiao Tong University, Shanghai 20040, China

<sup>3</sup> School of Agriculture, Food and Wine, University of Adelaide, Waite Campus, Urrbrae, South Australia 5064, Australia

<sup>4</sup> Key Laboratory of Crop Marker-Assisted Breeding of Huaian Municipality, Jiangsu Collaborative Innovation Center of Regional Modern Agriculture and Environmental Protection, Huaian 223300, China

**Keywords** Pollen · Microspore · Cell division · Ginseng · Reproductive development · Stages of anther development

## Introduction

In higher plants, male reproductive development is a complex biological process that includes stamen identity specification from the floral meristem, anther morphogenesis, and the formation of pollen grains via meiosis and mitosis within the flower (Wilson and Zhang 2009). Microsporogenesis and male gametogenesis within the anther are critical for alteration between diploid sporophyte and haploid gametophyte in flowering plants. Mature pollen grains (called microgametophytes) release sperm cells to the female reproductive structures for double fertilization, leading to the formation of seeds and/or fruits, which are essential for species survivals and agricultural production. To ensure successful male reproduction, the development of the somatic tissue, anther wall layers, and reproductive cells is tightly

coordinated (Zhao 2009; Feng and Dickinson 2010; Chang et al. 2011; Zhang et al. 2011; Kelliher et al. 2014; Zhang and Yang 2014).

Generally, the anther primordium that emerges from the floral meristem consists of three meristematic layers: the first layer forms the epidermis, the third layer forms the connective tissue, while the second layer differentiates into male reproductive cells (microsporocytes also called pollen mother cells, PMCs; or microspore mother cell, MMCs) and three inner somatic cell layers: the endothecium, the middle layer, and the tapetum (Zhang and Yang 2014). After morphogenesis of the anther, the anther is composed of four somatic layers surrounding the PMCs (Heslop-Harrison 1971; Bedinger 1992; Zhang et al. 2011).

Development of male reproduction has been investigated extensively in rice (*Oryza sativa*) (Raghavan 1988; Zhang and Wilson 2009; Zhang et al. 2011), *Citrus sinensis* (Koltunow et al. 1995), *Hibiscus syriacus* (Kim and Kim 1995), *Nelumbo nucifera* (Kreunen and Osborn 1999), *Arabidopsis* (*Arabidopsis thaliana*) (Sanders et al. 1999; Zhang et al. 2002; Zhao 2009; Feng and Dickinson 2010; Chang et al. 2011), *Bromeliaceae* (Sajo et al. 2005), *Onobrychis schahuensis* (Chehregani et al. 2008), *Carthamus tinctorius* (Yeung et al. 2011), and maize (*Zea mays* L.) (Kelliher et al. 2014). By contrast, few studies on anther development have been performed in the family *Araliaceae* even though there have been investigations on the morphological aspects of pollen grains. For example, the pollen grains of *Acanthopanax* (Tseng et al. 1983; Liu et al. 1998), *Aralia elata*, *Panax* genus, and *Oplopanax elatus* (Wen and Nowicke 1999; Jeong 2005; Reunova et al. 2007; Reunov et al. 2008), and *Trevesia burckii* (Gabarayeva et al. 2009a, b) on heteromorphism and metamorphosis have been reported.

*Panax ginseng* is a slow-growing perennial plant in the genus *Panax* L. in the family *Araliaceae*. Among the 17 *Panax* species, *P. ginseng*, known as Korean/Asian ginseng, followed by *P. quinquefolius*, known as American ginseng, are widely used for medicinal purposes. Ginseng root has been widely used as a health food and traditional medicine for thousands of years. Before harvesting, ginseng plants typically require cultivation for 4 to 6 years under shade conditions, which is challenging for efficient ginseng production because ginseng growth is susceptible to soil, climate, and shade perturbations as well as pathogens and pests (Lee et al. 2011; Oh et al. 2014). Propagation of ginseng plants is largely dependent on seeds produced via self-fertilization. The third year after seed generation, ginseng plants initiate flowering, and at the fourth year, the plants undergo active reproductive development with formation of 30–50 flowers attached on an umbel-type inflorescence. Additionally, although the origin and development of inflorescence architecture have received much attention (Zhang and Yuan 2014), little is known about reproductive development in *Panax* species. Therefore,

understanding the developmental events of ginseng plants, particularly their reproductive mechanisms, will help to improve ginseng production. In this study, we described the unique features on ginseng inflorescence and flower development. Particularly, we comprehensively investigated anther morphogenesis and pollen formation in *P. ginseng* together with morphological changes of the inflorescence in comparison with the previous reports on *Panax* genus and its close genera *Aralia* and *Acanthopanax* (Tseng et al. 1983; Wen and Nowicke 1999; Jeong 2005; Reunova et al. 2007; Reunov et al. 2008). This work will serve as the baseline knowledge for future investigations on ginseng reproduction.

## Materials and methods

### Plant growth

Fresh inflorescence and floral buds (also called as umbel) of 4-year-old cultivated *Panax ginseng* were collected from the ginseng field of Kyunghee University (South Korea) from the middle of April to end of May (15, 18, 22, 25 April and 2, 9, 13, 20 May), 2014. The length of stem, peduncle, and pedicle, the number and size of flowers were measured from 10 individual plants in each sampling time. The stage of anther and pollen development were determined by the length of anther measured by Olympus microscope BX61.

### Light microscopy for semi-thin section

The ginseng inflorescences at various stages were fixed using formalin-acetic acid alcohol (FAA, 50 % ethanol, 5 % glacial acetic acid, 3.7 % formaldehyde). The fixed samples are dehydrated in a graded ethanol series (70, 80, 90, and 100 %) during 30 min for each steps, and then embedded in KULZER's Technovit 7100 cold polymerizing resin (Heraeus Kulzer GmbH Philipp-Reis-Straße 8/13, D-61273 Wehrheim/Ts) by three steps of prefiltration, infiltration, and embedding at 45 °C (Igersheim and Cichocki 1996; Beeckman and Viane 2000; Zhang et al. 2013). Embedding samples were sectioned as 3–4 µm in thickness using an Ultratome III ultramicrotome (LKB) and stained with 0.25 % toluidine blue O (Chroma Gesellschaft Shaud) at 42 °C. Bright-field photographs of the anther sections were taken using a Nikon ECLIPSE 80i microscope and a Nikon DXM1200 digital camera.

### In situ hybridization

Samples were fixed in FAA and 2.5 % glutaraldehyde in 0.1 M sodium phosphate buffer, then dehydrated in a graded ethanol series (85, 90, 95, 100 %), replaced with xylen and embedded in Paraplast Plus (Oxford Labware). Microtome

sections (4  $\mu\text{m}$  thick) were placed onto slide glasses. Ginseng homologous ginseng gene of rice anther-specific gene *CYP703A3* (Yang et al. 2014) was analyzed using the genomic DNA sequence retrieved from ginseng genome database (<http://im-crop.snu.ac.kr/new/index.php>). The ginseng genome database was constructed as a part of on-going ginseng genome project (Next-Generation BioGreen 21 program No. PJ008202) in Korea. The full-length PgCYP703A cDNA is prepared from RNA isolated from ginseng flowerbud then cloned to pJET clone vector. Transcription in vitro under T7 or SP6 promoter with RNA polymerase using the DIG RNA labeling kit (Roche) was prepared for the DIG-labeled antisense (forward primer, 5'-ATG GAT TTC ACC CTC CTC CTA-3; reverse primer, 5'-AGC TCA TGA GTT ATG TGC AT-3') or sense probes. In situ hybridization and immunological detection of the signals were performed as reported by Li et al. (2006).

### Scanning electron microscopy

For scanning electron microscopy (SEM) examination, inflorescences with different size were collected, fixed, and washed as the same procedure for semi-thin section except the dehydration using 20, 30, 40, 50, 60, 70, 80, 90, and 100 % ethanol, respectively. The duration of each step was 3 min. After the dehydration, samples were thoroughly dried at critical point temperature (Leica EM CPD300). Leica EM SCD050 ion sputter was used for Aurum coating with 5-nm thickness. Aurum-coated samples were observed with Hitachi S3400N scanning electron microscope.

### Transmission electron microscopy

For transmission electron microscopy (TEM) examination, anthers at different developmental stages were prefixed in 2.5 % glutaraldehyde solution in 0.1 M sodium phosphate buffer (pH 7.2) and postfixed in 2 % osmium tetroxide ( $\text{OsO}_4$ ) in same buffer at room temperature (Kim and Kim 1995; Li et al. 2006). The samples were then dehydrated through a graded series of ethanol and embedded in Epon 812 resins (Racich and Koutsky 1976). Ultrathin sections (70 nm, Leica EM UC7, Germany) were double-stained with 2 % (w/v) uranyl acetate and 2.6 % (w/v) lead citrate aqueous solution and then examined with a 120-kV Biology Transmission Electron Microscope (Tecnai G2spirit Biotwin, FEI, Oregon, USA).

## Results

### Inflorescence development

Ginseng plants usually produce flowers in the third growth year when the stem develops three compound leaves and each

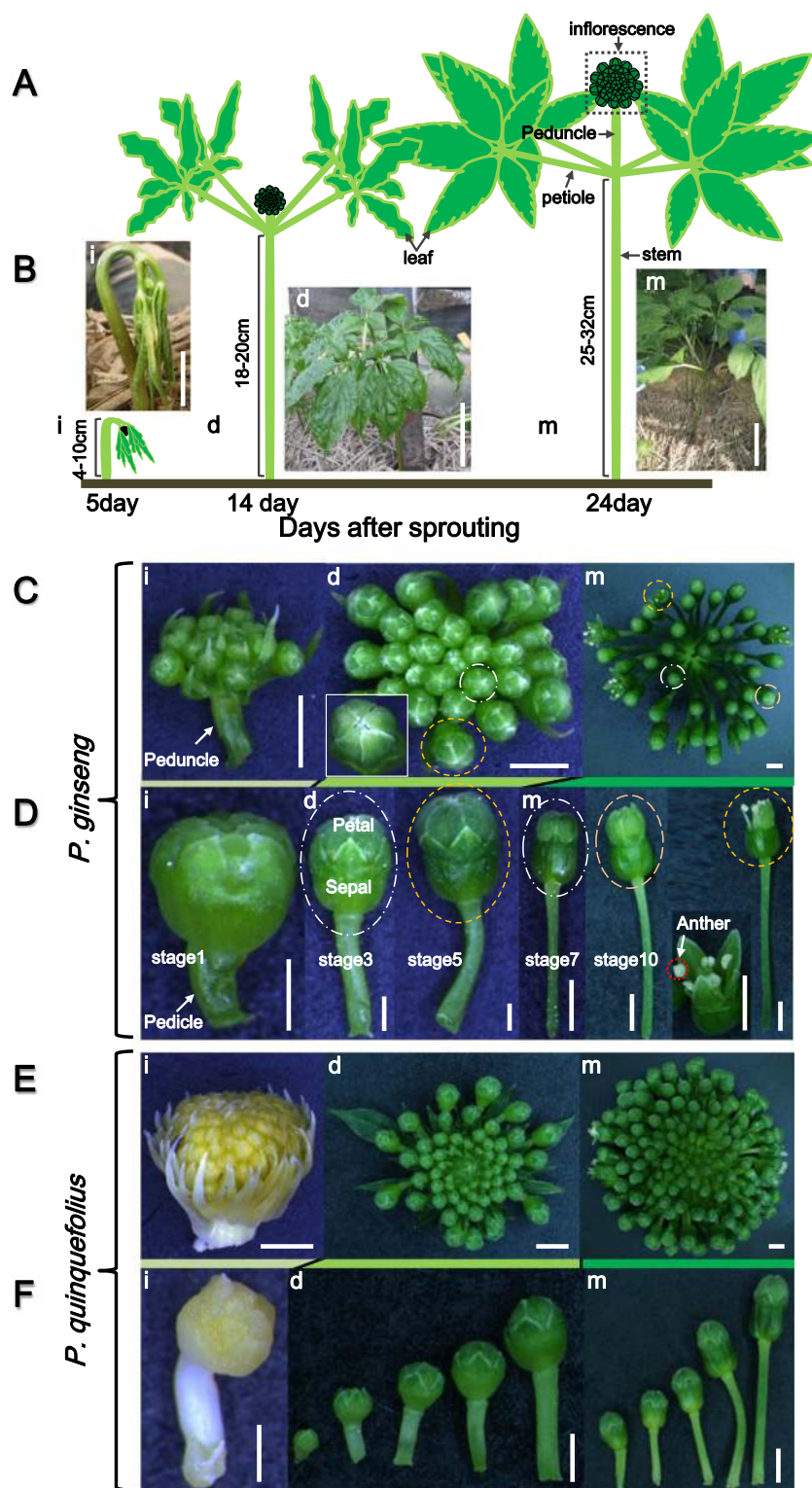
with five leaflets. In this study, we studied the inflorescence and flowers of 4-year-old *P. ginseng* cv. K1 because of active reproductive development and abundant flowers at this growth stage (Fig. 1). To correlate the developmental stages with the growth events, we measured the length of ginseng aerial parts, including the inflorescence and anther (Table 1, Fig. 1a, b). At the initial stage, the aerial parts exhibit a parasol-like shape (Fig. 1a(i), b(i); Kim et al. 2014), showing unfolded leaves attached to the bending stem, and an inflorescence primordia attached to a short peduncle (Fig. 1c(i)). Each inflorescence contained about 8–15 flower buds (Fig. 1c(i), c(d), d(i)) and small immature flower buds (about 1 mm) with a short pedicle (1–5 mm) gradually increased in size with maturation. Two weeks after sprouting, active growth of the stem and peduncle occurred, and leaves partially expanded (Fig. 1a(d), b(d)). During this developmental stage, the number of flowers increased to 20–45 per inflorescence (Fig. 1c(d)) and the pedicles of the outer flowers within the inflorescence were longer than those of the inner flowers (Fig. 1d(d)). At the mature stage, 3 weeks after sprouting, the height of the aerial parts was about 30 cm and leaves fully expanded (Fig. 1a(m), b(m)). Meanwhile, the peduncle (or inflorescence stalk) that arose from the shoot apical region kept a constant elongation and was finally located above the leaflets at the mature stage (Fig. 1c(m)). Furthermore, the multipedicelled umbel-shaped ginseng inflorescence had various sized flowers at this stage, ranging from closed flower buds to fertilized flowers (Fig. 1d(m)). About 1 month after sprouting, the pedicle linked with the calyx was as lengthen as the peduncle, and both pedicle and peduncle reached a maximum height of about 10 and 20 cm, respectively (Table 1).

Although the developmental events of the *P. quinquefolius* inflorescence appear similar to those of *P. ginseng*, *P. quinquefolius* had about 50–80 flower buds and pedicles, about two-fold more than *P. ginseng* (Fig. 1e). Moreover, unlike the green color of the *P. ginseng* inflorescence at the initial developmental stage, the inflorescence primordium of *P. quinquefolius* was pale yellow with a long involucre at this stage (Fig. 1e(i)). In addition, the variation in developmental stages of flower buds was more obvious in *P. ginseng* compared with *P. quinquefolius* (Fig. 1e(d), e(m), f(d), f(m)).

### Floral morphology

Each ginseng flower contained five sepals, five petals, and five stamens surrounding two stigmas (Fig. 2a–f). The sepals and their enclosed petals with fusion at the base in the immature flower bud at the initial developmental stage were green (Figs. 1d(i) and 2a). During growth, the individual petals became separated, with white visible at the apical region (Figs. 1c(d), d(d) and 2b). Sepals were dark green when the petals opened during fertilization (Figs. 1c(m), 1d(m) and 2c).

**Fig. 1** Inflorescence morphology at the different developmental stages of ginseng. **a** Cartoon showing *P. ginseng* morphology at the initial developing stage (*i*), the active developing stage (*d*), and the maturation stage (*m*) stage. **b** Pictures of *P. ginseng* plants in a ginseng field. Bars indicate 3 cm (*i*), 5 cm (*d*), and 10 cm (*m*), respectively. **c** Morphology of the *P. ginseng* inflorescence at three different stages. All bars indicate 2 mm. **d** Morphological changes in a single flower of *P. ginseng* with an elongated pedicle during the three different stages. Bars indicate 500  $\mu$ m (*i* and *d*) and 2 mm (*m*). **e** Morphology of *P. quinquefolius* inflorescence during three different developmental stages. All bars indicate 2 mm. **f** Morphology of a single inflorescence of *P. quinquefolius* during three different developmental stages. Bars indicate 500  $\mu$ m (*i*), 1 mm (*d*), and 2 mm (*m*)



Each stamen consisted of a pollen-producing anther subtended by a filament (Fig. 2g). During anther development, the color of the anthers changed from green at the initial stage to white during later stages (Fig. 2a–c), and the stomium was well developed during anther maturation (Fig. 2d, g, i). The anthers exhibited a butterfly shape in transverse sections

with four locules (Fig. 2i). Anther locules were connected by flanking connective tissue and vascular elements continuous with the filament (Fig. 2h, i). The ginseng anther was composed of two theca linked with connective and vascular tissues, and each theca contained two locules, with the outer part of the locule longer and larger than the inner one. The two

**Table 1** Major cell morphological and plant phenotype events during *P. ginseng* anther and pollen development

Stage events	Significant phenotype of plant	Anther length (mm)	Flower length (mm)	Pedicel length (cm)	Peduncle length (cm)	Plant height (cm)	Days after sprouting	Plant develop stage <sup>a</sup>	Rice stage <sup>b</sup>	Arabidopsis stage <sup>c</sup>
1 Cell division	Leaves are unfolded with very small inflorescence.	0.2–0.25	0.7–1.10	0.1–0.5	0.2–0.4	4–10	5~10	i	5	4
2 Cell division		0.30–0.50	1.08–1.45	0.5–1.0	0.5–0.8	10–15	10~14	i	6	5
3 Meiosis	Leaves are partially expand.	0.50–0.60	1.49–1.79	1.0–1.5	0.8–1.2	18–20	14	d	7	6
4 Tetrad	Five petals are fully isolated.	0.60–0.70	1.80–1.90	1.5–2.0	1.2–3.5	18–32	14~24	d	8	7
5 Young microspores	Plant grows fully and leaves are fully expanded.	0.70–0.80	1.88–2.07	4–5.5	4.0–7.0	25–32	24	d	9	8
6 Vacuolation		0.80–0.88	2.33–2.51	5.5–6.0	7.0–12	25–32	24~31	m	10	9
7 1st Mitosis	Anther color becomes whiter. Flower looks snowman shape.	0.88–0.93	2.33–2.65	6.0–9.0	7.0–12	25–32	24~35	m	11	10
8 2nd Mitosis		0.94–1.14	2.98–3.15	9.0–10	12–20	25–32	24~35	m	12	11
9 Maturing pollen		0.87–1.01	3.11–3.31	9.0–10	15–20	25–32	35~40	m	13	12
10 Matured pollen release	Flowers starts open and anther starts dehiscence.	0.87–0.94	3.49–3.56	9.0–10	15–20	25–32	35~45	m	14	13

<sup>a</sup> Plant developmental stage is followed by Fig. 1: i, initialing procedure; d, developing procedure; m, maturing procedure

<sup>b, c</sup> Anther stages of rice and *Arabidopsis* were followed by previous description by Zhang et al. (2011) and Sanders et al. (1999), respectively

locules were connected by the inner side of the anther wall (ISAW), a septum, and a stomium for anther dehiscence (Fig. 2i). The anther was white till maturity, and the pollen sac was full of matured pollen grains and ready for release them when the flowers open (Fig. 2g–i).

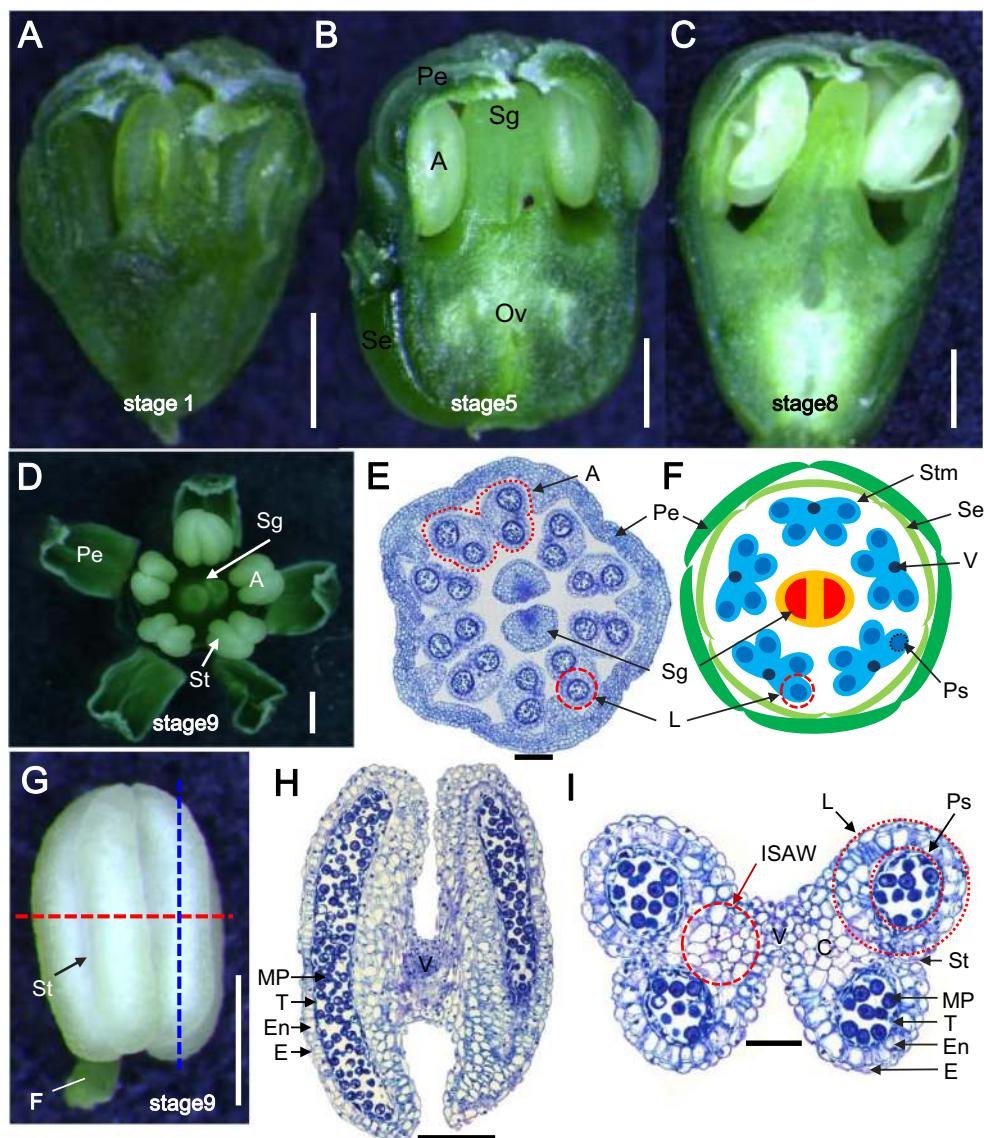
## Anther and pollen development

To understand cytological changes in *P. ginseng* during anther development and the formation of pollen grains, we employed semi-thin section analysis. Generally, within a single ginseng flower bud, anther and pollen development varied in stages among individual stamens. Furthermore, pollen development varied along the length of the individual anther. We divided anther and pollen development of *P. ginseng* into 10 stages at which distinctive cellular events could be visualized at the level of a light microscope (Fig. 3a). Table 1 summarizes the key events that occurred during the 10 stages of anther development.

After cell division and differentiation of the floral meristem, which contained layer 1 (L1) and L2, L1 cells within the anther primordium divided to form the epidermis and stomium, while two secondary parietal layers and sporogenous cells formed from L2 (Fig. 3a(1)). We defined this stage as stage 1, during which anther length ranged from 0.2 to 0.25 mm. The outer secondary parietal layer generated the endothecium layer and the middle layer, and the inner secondary parietal layer developed into the tapetal layer (Fig. 3a(1)). At stage 2, four formatted concentric somatic layers surrounded the sporogenous cells: the epidermis, the endothecium, the middle layer, and the tapetal layer from outer to inner, and obvious nuclei were observed in these anther wall layers (Fig. 3a(2), (8)), suggesting active cell division. Remarkably, the endothecium and the tapetum of the anther wall opposite the central vascular tissues comprised a single cell layer each, respectively. In contrast, the endothecium of the ISAW had one to four cell layers while the tapetum comprised one to two layers. Furthermore, the cell arrangement of the tapetal layer appeared uneven (indicated by stars and arrows in Fig. 3a(2)), suggesting unsynchronized cell division of secondary parietal layers for the generation of endothelial and tapetal cells. In addition, at this stage, the middle layer only had one cell layer and appeared well developed, the sporogenous cells formed by cell division from the precursor cells within the central space of the anther had increased in number and had densely stained cytoplasm and obvious nuclei (Fig. 3a(2)).

During morphological expansion of ginseng leaves at stage 3 (Fig. 1a(d), b(d)), there was further differentiation of the anther wall layers, epidermal cells appeared uneven, and the middle layer became thin, suggesting the initiation of cell degeneration (Fig. 8). Furthermore, the tapetal layer appeared

**Fig. 2** Morphology of a single flower of *P. ginseng* showing the floral organs and anther section. **a** Immature flower with unmatured green anthers at the initial developmental stage. **b** A flower with a clear ovary and anthers at the developing stage. **c** A mature flower with white anthers at the mature developing stage. All bars indicate 500  $\mu\text{m}$ . Opened flower (**d**), transverse section (**e**), and cartoon (**f**) show the formation of five mature anthers and two stigmas. Bars indicate 500  $\mu\text{m}$  (**d**) and 200  $\mu\text{m}$  (**e**). The mature anther has a white appearance and is attached to the filament (**g**), longitudinal section (**h**), and transverse section (**i**). Bars indicate 500  $\mu\text{m}$  (**g**) and 200  $\mu\text{m}$  (**h**, **i**). Two sections of the anther at stage 7 showing the anther wall layers, microspores in the locule, as well as vascular tissues and connective tissues at the ISAW. *A* anther, *Stm* stamens, *Ov* ovary, *Se* sepal, *Pe* petal, *Sg* stigma, *Ps* pollen sacs, *V* vascular bundle, *T* tapetum, *En* endothecium, *MP* mature pollen, *E* epidermis, *F* filament, *L* locule, *St* stonium; *ISAW* inner side of the anther wall



larger and more irregular in cell shape, and MMCs formed from sporogenous cells initiate meiotic division (Fig. 3a(3)).

At stage 4, when the flower bud had fully separated sepals (indicated by the box in Fig. 1c(d)), the middle layer was almost fully degraded, and tapetal cells started the condensation with dark-stained cytoplasm, an indicator of cell degeneration triggered by programmed cell death (PCD). At this stage, MMCs continue the process of meiosis II with the formation of tetrads, consisting of four newly generated haploid microspores enclosed by a callose wall deposited on the primexine of the microspore (Fig. 3a(4), (8); Supplementary Fig. S1B).

At stage 5, as the stem grew with fully expanded leaves and the peduncle elongated (Fig. 1a(m), b(m)), free haploid young microspores were released from the tetrads, the endothecium and tapetal cells became vacuolated, and the tapetal layer continued to degenerate as young microspores developed

(Fig. 3a(5), (8)). At stage 6, the microspores increased in size through vacuolation, the endothecium became enlarged, and the tapetum continued to degenerate with much condensation (Fig. 3a(6)). At stage 7, the anther appeared white, and vacuolated microspores initiated the first mitosis with asymmetric cell division, giving rise to a much smaller generative cell and a larger vegetative cell. Meanwhile, the endothecium underwent secondary thickening (Fig. 3a(7)). At stage 8, when the pedicle and peduncle were the most elongated, the bicellular pollen grain underwent a second round of mitosis, and the endothecium contained expanded cells with thick cell walls, while tapetal cells formed a band-like structure (Fig. 3a(8)).

At stage 9, mature spherical pollen grains full of storage starch formed. The middle layer and the tapetum had completely degenerated by this stage with tapetum-derived remnants, leaving the epidermis and the endothecium



**Fig. 3** Cytological observation and diagrams of *P. ginseng* anther development and pollen formation during the 10 developmental stages. **a** Anther sections were stained with toluidine blue and photographed by bright-field microscopy. Stages of anther development were observed in each locule. Anther cell layers differentiated into epidermis (E, yellow), endothecium (En, sky blue), middle layer (M, purple), and tapetum (T, pink). Irregular cell division of endothelial and tapetum cells are indicted by the *arrows* and *asterisks*, respectively. All bars indicate 50  $\mu\text{m}$ . **b** Diagram of cell lineages during anther development in the inner sides of the anther wall (ISAW) and outer sides of the anther wall (OSAW). 2'P secondary parietal cell layer, E epidermis, En endothecium, T tapetum, M middle layer, *Tds* tetrads, *MMC* microspore mother cell, *Msp* microspore, *MP* mature pollen, *SP* sporogenous cell, *St* stomium

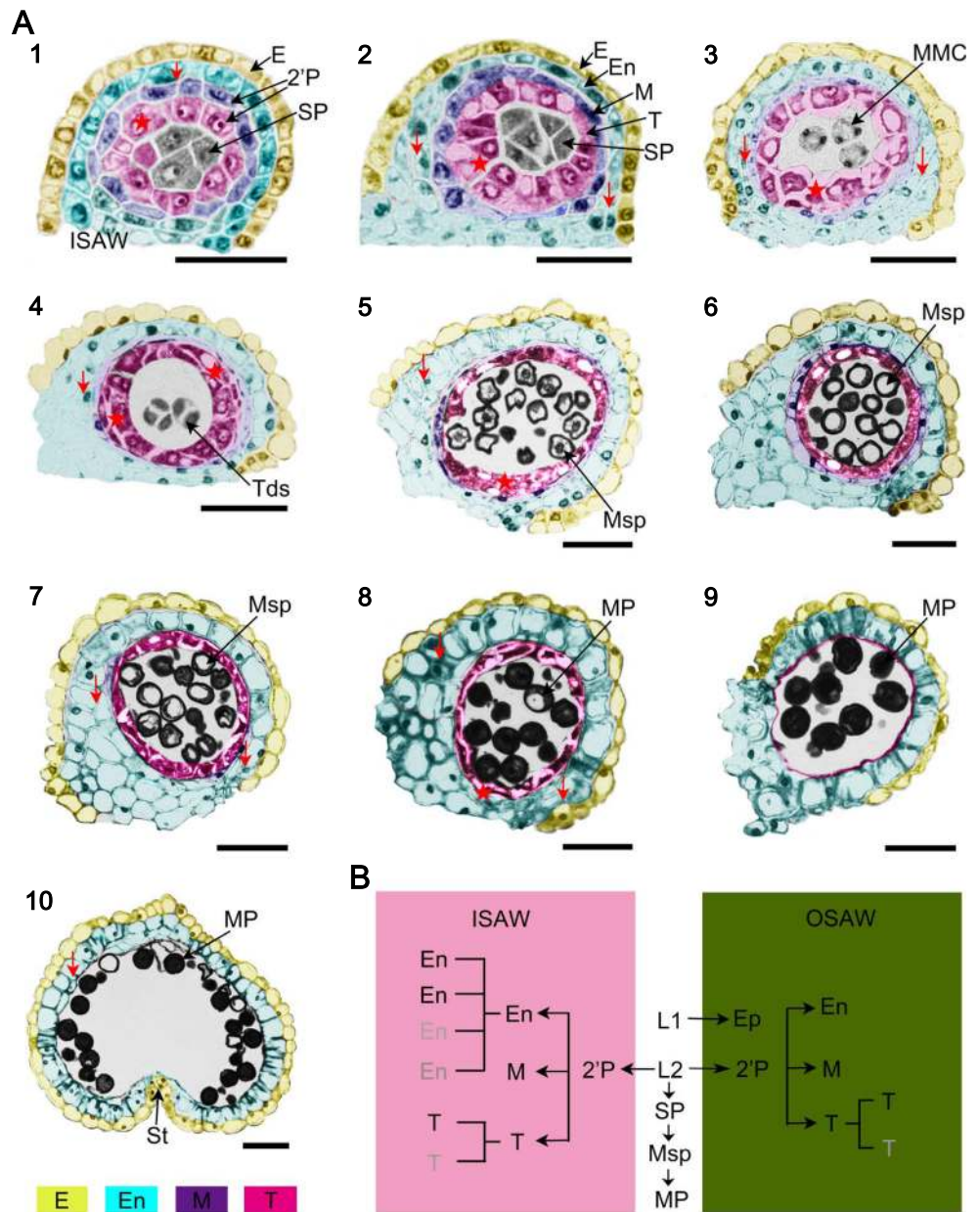


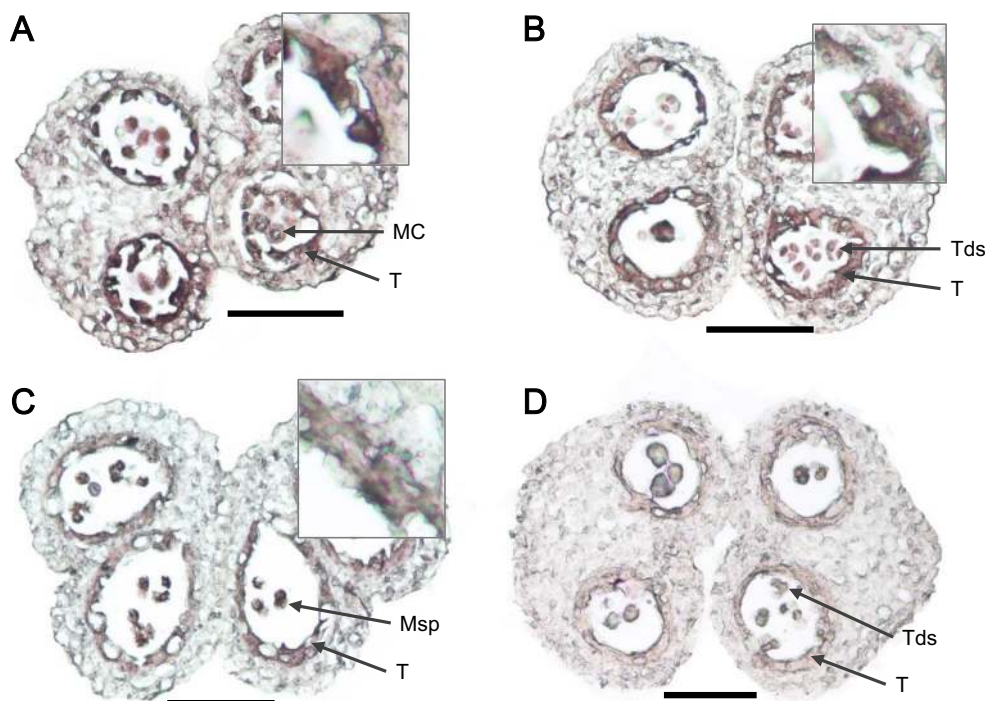
(Fig. 3a(9)). At stage 10, the anther started to dehisce by breakage of the stomium, leaving behind the epidermis and endothecium layers. Tapetal cells were completely degraded and the two adjacent pollen sacs combined. The septum connecting the two pollen sacs broke, and anther walls at the stomium region located between the two locules started to break to release matured pollen grains by dehiscence (Fig. 3a(10), (8)).

### In situ analysis

The above light microscopic analysis revealed uneven cell division of the endothecium and tapetal layers. To further characterize the cell identity of these cell layers, we cloned a

DNA fragment called *PgCYP703* identified from the ginseng genome database. *PgCYP703* shares 93 % identities with rice *CYP703A3* (Yang et al. 2014) and *Arabidopsis CYP703A2* (Morant et al. 2007), which are expressed in tapetal cells during pollen development. Further, the expression of *CYP703A3* is regulated by tapetum degeneration retardation (TDR) (Li et al. 2006; Yang et al. 2014) and *GAMYB* (Aya et al. 2009), two known regulators of tapetal PCD and pollen exine formation, respectively, in rice. Results of in situ hybridization using *PgCYP703* showed high expression in one to two layers of tapetal cells of the anther during the formation of tetrads (Fig. 4), confirming our assumption that ginseng anther undergoes uneven cell division during anther wall formation. Due to the lack of a marker gene for the endothecium, cells

**Fig. 4** Expression of *PgCYP703* during anther development. In situ analysis of *PgCYP703* in *P. ginseng* anther at stage 3 (a), stage 4 (b), and stage 5 (c) showing expression of *PgCYP703* (dark pink) in tapetal cells and microspores. The enlarged section is boxed on the top right of a, b, and c. Stage 4 (d) hybridized with the *PgCYP703* sense probe. All bars indicate 500  $\mu\text{m}$ . T tapetum, Tds tetrads, MMC microspore mother cell, Msp microspore



associated with the endothecium were not characterized at the molecular level.

### TEM analysis of anther development

To precisely observe subcellular changes associated with anther development and pollen formation, we conducted TEM analysis (Fig. 5). During the anther cell wall differentiation stage, the outer secondary parietal cells divided into the endothecium and middle layer, the inner secondary parietal cells developed into the tapetal layer (Fig. 5a, b), and the central localized sporogenous cells differentiated into MMCs at stage 3 (Fig. 5c). MMCs contained numerous mitochondria and rough endoplasmic reticulum (ER) with expanded cisternae (Supplementary Fig. S3). Remarkably, during differentiation and development of the ginseng anther, tapetal cells became vacuolated and two-fold larger in size than the other anther wall cells. Consistent with the above observations based on examination of semi-thin sections and in situ analysis (Figs. 3 and 4), uneven cell division was also observed in the tapetum and the endothecium as evidenced by the presence of one or more layers of these cells in one anther (indicated by stars and arrows, respectively, in Fig. 5a–d). At stage 3, the tapetal cells appeared well differentiated and could be clearly distinguished from the other anther wall cell types by their dense cytoplasm (Fig. 5c, d). The middle layer also became very thin (Fig. 5d).

The mature anther wall consisted of dehydrated epidermal cells with a surface cuticle and expanded endothecium cells with secondary wall thickening (Fig. 5e, g). Although the

tapetum degraded in the mature anther, tapetum-derived pollen remnants were still present in the periphery of the locule, filling the cavities of a sporopollenin-based exine framework of tricellular pollen, completing pollen wall formation (indicated by the arrowheads in Fig. 5h). Ginseng tapetum appeared to be a secretory-type tapetum that produces granule structures (called orbicules) with dark-staining during TEM analysis (Fig. 5f, h). The orbicules developed simultaneously from stage 7 to stage 9 during pollen exine development (Supplementary Fig. S4).

Each mature tricellular pollen grain possessed two gametes in the parietal position, and each had a prominent nucleus at stage 8 (Fig. 5f). During the maturation of a pollen grain, the outer pollen wall, called the exine, became well established as the synthesis, deposition, and assembly of sporopollenin precursors (Fig. 3a(5)). The formation of ginseng exine seems to be initiated from the tetrad stage (stage 4) through primexine formation and undulation of the plasma membrane. Young microspores released from the tetrad started to develop baculum, which is the vertical element in the pollen wall, nexine, and tectum (Fig. 7a–d) that gives mature pollen with the appearance of a fine reticulum (Fig. 7e–h). During maturation of pollen grains, there was differentiation between nexine I and nexine II (Fig. 7c, d, g, h). After complementation of exine development, the intine, which is pecto-cellulosic in nature, developed as a thin layer after active development of high electron-dense organelles at the periphery of the pollen grain cytoplasm (Fig. 7d). Finally, mature pollen grains were characterized by a well-developed exine

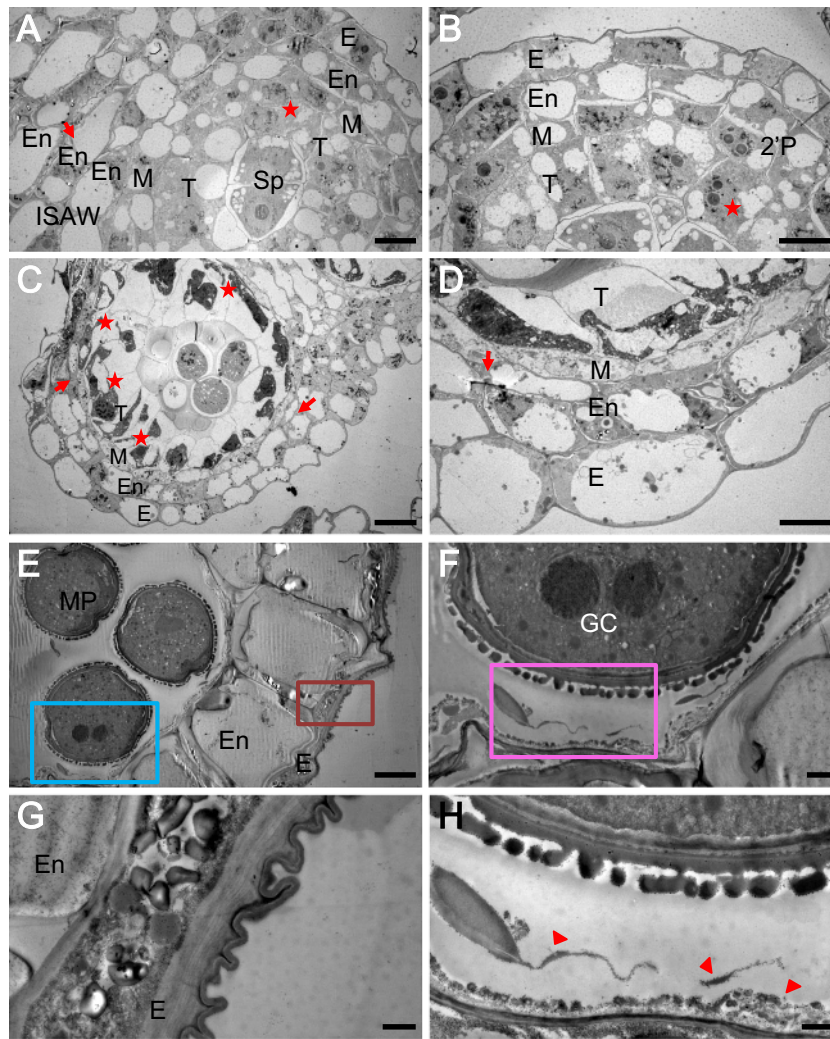


**Fig. 5** Transmission electron micrographs of *P. ginseng* anthers at different developmental stages. Somatic cells differentiated into six layers in the inner sides of the anther wall (ISAW) (a) and four layers in the outer sides of the anther wall (OSAW) (b) within a single anther locule at stage 1. Irregular cell division of endothelial and tapetal cells is indicated by arrows and asterisks, respectively. Bars indicate 10  $\mu\text{m}$ . Anther at stage 3 was characterized by four differentiated layers with irregular division (c) and a high cell density (d) of tapetal cells. Bars indicate

20  $\mu\text{m}$  (c) and 10  $\mu\text{m}$  (d). Anther at stage 9 had a thin epidermis with the formation of a cuticle, thickened endothecium (e, g), and one mature pollen grain with two generative cells (GC) (f). Pollen grain had an established exine in contact with orbicules (indicated as arrows) from complete degenerated tapetal cells (h). Bars indicate 10  $\mu\text{m}$  (e), 2  $\mu\text{m}$  (f), and 1  $\mu\text{m}$  (g, h). E epidermis, En endothecium, M middle layer, T tapetum, MP mature pollen, ISAW inner sides of anther wall, SP sporogenous cell, 2'P secondary parietal cell layer

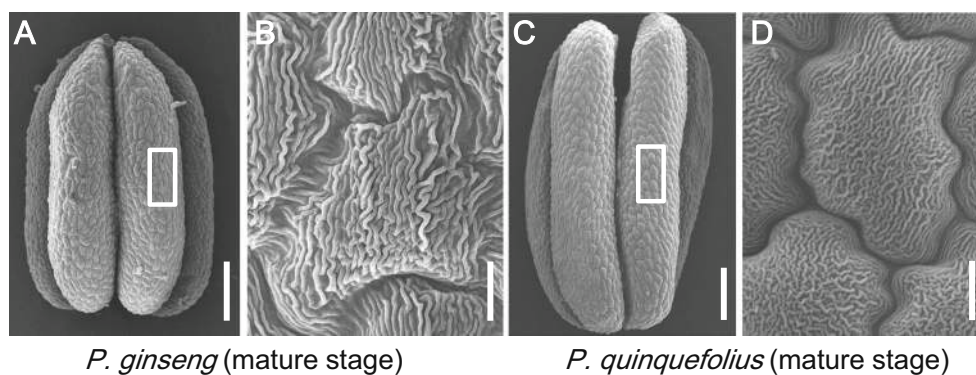
comprising a uniformly thick nexine I (0.7  $\mu\text{m}$ ), thin nexine II (0.1  $\mu\text{m}$ ), and sexine (1  $\mu\text{m}$ ) (Fig. 7g). The sexine consisted of a tectum (0.5  $\mu\text{m}$ ) linked by an irregular bacula (0.1–0.5  $\mu\text{m}$ ) and pollen coat (Fig. 7g). Usually, the thin layer of intine (0.4  $\mu\text{m}$ ) between the exine and cytoplasm plasma membrane in the non-apertural region of the pollen had a lower density than the exine (Fig. 7g, i), but the intine was up to 3  $\mu\text{m}$  thick in the apertural region (Fig. 7h).

### Features of ginseng anther and pollen morphology

The anthers of *P. ginseng* and *P. quinquefolius* had obvious lobe boundaries (Fig. 6a, c), and their anther cuticle displayed

striated patterns (Fig. 6b, d), whereas ginseng cells had a smoother appearance at early developmental stages (Supplementary Fig. S2). In addition, ginseng anthers contain various pollen grains with an average size of 20  $\mu\text{m}$ , ranging from 16 to 27  $\mu\text{m}$  (Reunova et al. 2007) (Fig. 7e). Mature pollen grains of ginseng are tricolpate and reticulate due to the external tectum structure (Fig. 7e, f). Even though *P. ginseng* and *P. quinquefolius* are the closest species in the same genus, minor differences in the pollen structure were evident between them: *P. ginseng* pollen grains had thick, almost continuous tecta and an infratectum comprising a short bacula and sparse granules, whereas pollen of *P. quinquefolius* had a thinner, discontinuous, and weakly striato-reticulate tectum, similar to previous report (Wen and Nowicke 1999).

**Fig. 6** Characterization of the outer surface of ginseng anthers compared with those of *Arabidopsis* and rice by scanning electron microscope. **a** *P. ginseng* anther at stage 9, *bar*=200  $\mu$ m. **b** Enlargement of **a** showing the anther cuticle, *bar*=10  $\mu$ m. **c** *P. quinquefolius* anther at stage 9, *bar*=200  $\mu$ m. **d** Enlargement of **c** showing the anther cuticle, *bar*=10  $\mu$ m



**Discussion**

Despite the long history of the use of ginseng in medical applications, little is known about its reproduction. Development of the inflorescence and flower structure is essential for plant survival and agricultural yield. In this paper, we performed detailed observation on ginseng inflorescence and flower morphology and comprehensive cytological analysis of ginseng male reproductive development. Furthermore, the anther developmental process is grouped into ten stages based on cytological events. In addition, the common and

specialized developmental features in ginseng are addressed in comparison with other model plants.

**Characteristic morphology of ginseng inflorescence and flowers**

Flower morphology of the family *Araliaceae* is extremely diverse, in contrast to low variation of mature flower structure of Umbelliferae, which is closely related family of *Araliaceae* (Nuraliev et al. 2010). *Panax* L. has a single terminal inflorescence with an umbel shape, in contrast to other species in the

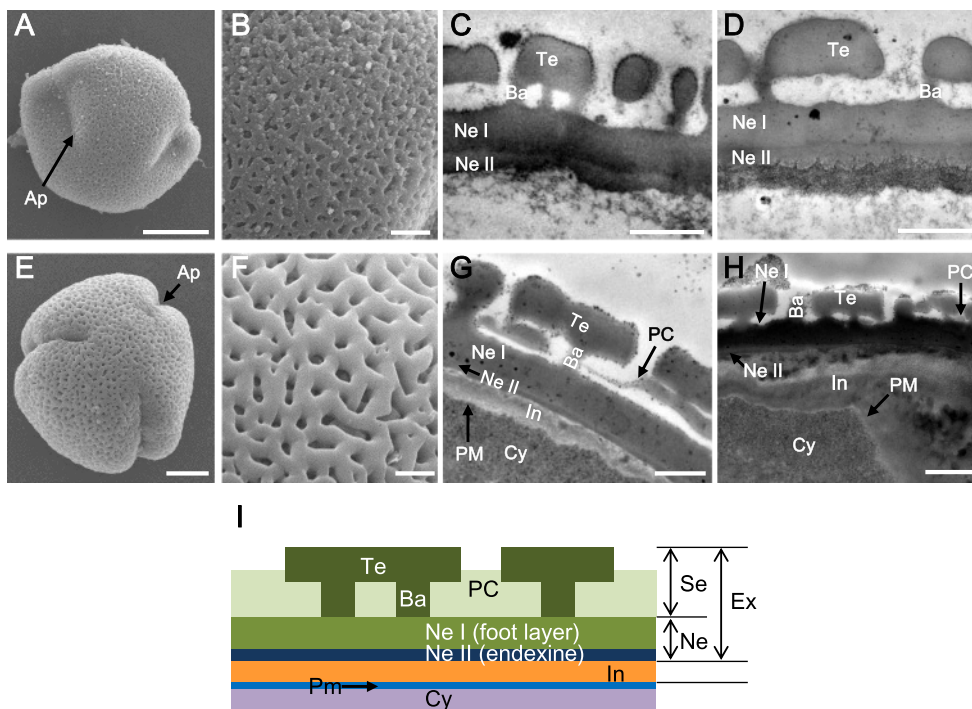


**Fig. 7** Pollen grain and pollen wall morphology analysis of *P. ginseng* at stage 5 (**a–d**) and stage 9 (**e–h**). Outer appearance of pollen grain (**a**), enlargement of pollen grain surface (**b**) by SEM, and pollen wall section by TEM (**c**, **d**) showing a less reticular structure than that of *Arabidopsis*. At this stage, bacula (Ba), tectum (Te), and nexine I (Ne I) were apparent, whereas the nexine II (Ne II), which was difficult to distinguish in **c**, further developed during development of pollen grain with highly electron-dense cells at the periphery of the cytoplasm (**d**). Mature pollen

grains had a rough outer appearance (**e**) and showed enlargement of the pollen grain surface (**f**) by SEM, while the pollen wall had a reticular structure as determined by TEM (**g**, **h**). Pollen grain had a thin intine at nonaperture regions (**g**) and a thick intine at the aperture region (**h**). Bars indicate 5  $\mu$ m (**a**, **e**), 1  $\mu$ m (**b–d**, **f–h**). **i** Diagram of ginseng pollen exine structure. *Te* tectum, *Ba* bacula, *PC* pollen coat, *In* intine, *PM* plasma membrane, *Cy* cytoplasm

family *Araliaceae*, while *Panax trifolius* and the nearest genera *Aralia* have multiple inflorescences for each plant. Among *Panax* L., two major important species, *P. ginseng* and *P. quinquefolius*, are closely related and more advanced species (Wen and Nowicke 1999). In ginseng plants, the transition from vegetative growth into reproductive growth frequently occurs in the second growth year when the plant produces at least two compound leaves with petioles in each stem. During third growth year, the indeterminate inflorescence attached by a single peduncle developed from the primordium forms from second-year growth plants. Unlike studies in annual plants which have multiple axillary meristems originated from the shoot apical meristem during inflorescence and flower development (Zhang and Yuan 2014), ginseng plant usually produces a single inflorescence from the primordium contained within the underground bud of a rhizome formed during June to August of the previous year (Baranov 1966; Thompson 1987; Kim et al. 1998). The feature of ginseng in producing the inflorescence primordium in the previous year and requiring winter dormancy for further development of inflorescence is a characteristic of perennial plants (Meloche and Diggle 2003; Albani and Coupland 2010). Furthermore, we observed the cell differentiation from sporogenous cells into pollen mother cells after dormancy in ginseng, which is similar to that in other woody perennial plants (Boss and Strauss 1994; Julian et al. 2011). However, the mechanism underlying this switch still remains elusive. Furthermore, each ginseng flower has five green petals, and the upper region of the petals is white in color, with each petal surrounded by depressed sepals. The specialized flower structure of ginseng might be due to adaptation to the environmental factors and selection for pollination. The characteristic inflorescence and flower development imply tight regulation of genetic and environmental factors during acquisition of meristem identity, which remain to be investigated in the future.

### Nonsynchronous development of ginseng anther wall layers

To facilitate research on ginseng male reproduction, we grouped the development of the ginseng anther into 10 stages based on cytological observations and the length of the anther (Table 1). Overall, the development of the ginseng anther ranging from anther primordium formation, anther wall, reproductive cell division, differentiation to pollen formation, maturation, as well as anther dehiscence, appears to be a well-conserved process in angiosperms, suggesting conserved control of male reproduction in higher plants. After morphogenesis, each ginseng anther contained four anther wall layers, i.e., the epidermis, the endothecium, the middle layer, and the tapetum surrounding the male reproductive cells. After meiosis, the middle layer and the tapetum degraded, likely promoted by PCD (Fig. 8). Expansion and secondary wall thickening

in the endothecium layer and disappearance of the tapetum and middle layer, which were observed at stage 9, is essential for pollen dispersal by anther dehiscence along specialized cells of the epidermis (Mitsuda et al. 2005; Yang et al. 2007).

Interestingly, unlike uniform anther wall layers such as the tapetal layer in rice and *Arabidopsis* (Sanders et al. 1999; Zhang et al. 2011; Quilichini et al. 2014), we observed nonsynchronous development of ginseng anther wall layers, particularly the endothecium and the tapetum, during early anther development. Large number of middle layers also have been observed in other woody plants such as *Populus bolleana* and *Prunus armeniaca* (Zhang et al. 2009; Julian et al. 2011), which would contribute for thick anther walls. However, tapetum is a usually uniseriate, rarely multiseriate in few plants from *Poaceae* and *Cucurbitaceae* family and *Peperomia* genus (Fisher 1914; Nakamura et al. 2010; Pandey et al. 2014). In *Araliaceae* family, it was also shown at least two layer of tapetum and uneven cell division during tetrad stage of *T. burckii* microspore (Gabarayeva et al. 2009a). It will be interesting to investigate the mechanism underlying the formation of multiple tapetal layers.

From stages 1 to 4, anther parietal cells in *P. ginseng* differentiated into four anther cell walls, and the outer secondary parietal cell layer divided periclinally to form the middle layer and the endothecium, while the inner secondary parietal layer differentiated into tapetal cells (Supplementary Fig. S1A). Notably, nonsynchronous cell division occurred during formation of the tapetum and the endothecium, as evidenced by the observation of two to four layers in the ISAW, and one layer of tapetum and endothecium near the outside of the anther wall (OSAW), respectively (Figs. 3a, stages 1–3, b, 4a, b). The identity of tapetal cells was confirmed by in situ analysis using *CYP703* homolog in ginseng as a probe (Fig. 4) (Yang et al. 2014). Due to the lack of a specific marker gene for the endothecium (Zhang et al. 2011; Zhang and Yang 2014), we were not able to determine the cell identity of the endothecium. Nonsynchronous cell division to generate anther wall layers, particularly of tapetal cells, has not been observed in *Arabidopsis* and rice (Sanders et al. 1999; Zhang et al. 2011; Quilichini et al. 2014). Recently, tapetum multilayer was observed as associated with male sterility in maize (Chaubal et al. 2000), tomato (Sawhney and Bhadula 2011), and *Arabidopsis* (Cecchetti et al. 2015), confirming the important role of tapetum in normal pollen development regulated by auxin transportation. This feature suggests a specialized developmental program for ginseng anther wall development, which remains to be investigated.

Successful formation of pollen grains relies on nutritive support from the neighboring somatic tissue, i.e., the tapetal cells. Upon degeneration of tapetal cells, nutrients such as lipidic molecules and sugars produced within tapetal cells are transferred across the tapetal cells for pollen wall development (Li and Zhang 2010). However, ginseng tapetum

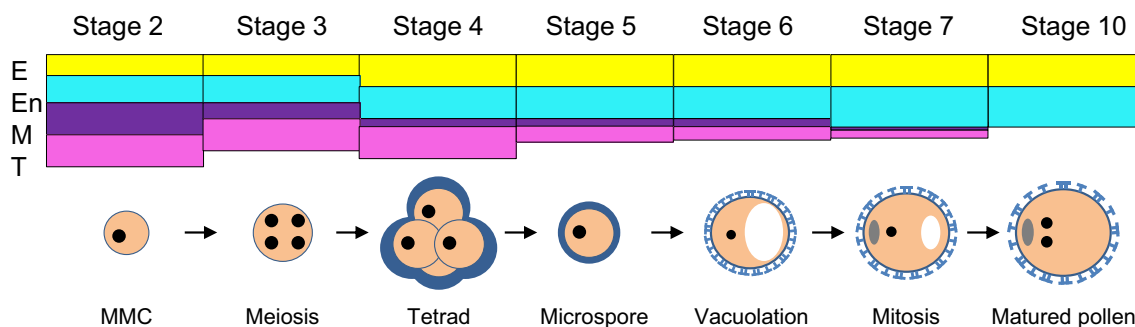


**Fig. 8** Schematic model of pollen and anther wall development in *P. ginseng*. Anther somatic cell wall of *P. ginseng* at stage 2; four distinct cell layers were evident: epidermis (E, yellow), endothecium (En, sky blue), middle layer (M, purple), and tapetum (T, pink). Epidermis and endothecium became thicker at the tetrad stage of the

microspore (stage 4), whereas the middle layer became thinner due to meiosis of the microspore mother cell (stage 3) and finally disappeared after vacuolation of the microspore (stage 6). After pollen mitosis, the tapetum degenerated, whereas the endothecium became thicker (stage 7)

degeneration exhibited a little delay compared with other reported species of angiosperms in which their tapetal cells begin to degeneration before the tetrad stage (Sanders et al. 1999; Parish and Li 2010; Zhang et al. 2011). The inner side of tapetal cell has the attached orbicule-like structures pending in the locular fluid (Fig. 5h; Supplementary Fig. S4), which was also identified from *T. burckii* in the *Araliaceae* family (Gabarayeva et al. 2009b). These granule structures on the tapetum may play a key role in regulating the development of pollen exine, which is similar to that of Ubisch bodies/orbicules on the inner surface of tapetal cells in cereal plants, such as rice and wheat (Huysmans et al. 1998; Li and Zhang 2010), or tapetosomes in *Arabidopsis* and elaioplasts in *Brassicaceae*, assumed to export tapetum-produced sporopollenin precursors across the hydrophilic cell wall to the locule (Wu et al. 1997; Furness and Rudall 1998; Quilichini et al. 2014).

### Pollen wall structures in ginseng

The pollen wall, surrounding the sperm cells, functions as a protective barrier for sperm cells and confers resistance to environmental stresses after anther dehiscence (Blackmore et al. 2007; Li et al. 2010; Li and Zhang 2010; Shi et al. 2011). Development of the pollen wall in ginseng is obvious from the early tetrad stage (stage 4) and almost completes at the maturing pollen stage (stage 9), consistent with previous observations (Jeong 2005). Compared with other plants, the *P. ginseng* exine has a shorter bacula and thicker nexine, which are commonly characteristics of most *Panax* species, except *Panax trifolius* (Wen and Nowicke 1999). It could be caused by high accumulation of pollen wall exine, comparable with less accumulation in close genus, *Aralia* (Reunov et al. 2008). The structural characteristics of pollen wall, reticulate cavities with an abundant pollen coat inside the pollen exine, may be associated with pollination habits, such as insect pollination (Zhang et al. 2011). Moreover, *P. ginseng* has thicker, almost continuous tecta (Fig. 7), whereas *P. quinquefolius* has

thinner, and discontinuous, and weakly striato-reticulate tectum (Wen and Nowicke 1999).

In short, we described the characteristic development of the inflorescence and flower of *P. ginseng* and performed comprehensive cytological analysis of ginseng anther development and pollen formation. Furthermore, we categorized the developmental stages of the ginseng anther into 10 stages on the basis of biological events. Determination of the mechanism controlling nonsynchronous cell division within anther wall layers such as the tapetal layer in the same anther lobe is an interesting topic for future research. The information provided in this study will benefit fundamental research on ginseng reproductive development as well as plant breeding and male fertility manipulation.

**Acknowledgments** We express our thanks to Dr. Jakyung Lee, Professor Gynheung An (Kyung Hee University) for comments about flower sampling and fixation and Li Yang, Junping Yu, and Dr. Jie Xu (Shanghai Jiao Tong University) for comments about flower section. This work was supported by the funds from Ministry of Science and Technology (2015DFG32560), and the Programme of Introducing Talents of Discipline to Universities (111 Project, B14016), Young Scientist Exchange Program between Republic of Korea (NRF) and The People's Republic of China (MOST) and NRF (2013R1A1A2064430) (YJ Kim); and Korea Institute of Planning and Evaluation for Technology in Food, Agriculture, Forestry and Fisheries (iPET; 112142-05-1-CG000), Republic of Korea (DC Yang).

**Conflict of interest** The authors declare that they have no conflict of interest.

### References

- Albani MC, Coupland G (2010) Comparative analysis of flowering in annual and perennial plants. *Curr Top Dev Biol* 91:323–348
- Aya K, Ueguchi-Tanaka M, Kondo M, Hamada K, Yano K, Nishimura M, Matsuoka M (2009) Gibberellin modulates anther development in rice via the transcriptional regulation of GAMYB. *Plant Cell* 21(5):1453–1472

- Baranov A (1966) Recent advances in our knowledge of the morphology, cultivation and used of ginseng (*Panax ginseng* C.A. Meyer). *Econ Bot* 20(4):403–406
- Bedinger P (1992) The remarkable biology of pollen. *Plant Cell* 4(8): 879–887
- Beeckman T, Viane R (2000) Embedding thin plant specimens for oriented sectioning. *Biotech Histochem* 75(1):23–26
- Blackmore S, Wortley AH, Skvarla JJ, Rowley JR (2007) Pollen wall development in flowering plants. *New Phytol* 174(3):483–498
- Boss TK, Strauss SH (1994) Floral phenology and morphology of black cottonwood. *Populus trichocarpa* (Salicaceae) *Am J Bot* 81:562–567
- Cecchetti V, Brunetti P, Napoli N, Fattorini L, Altamura MM, Costantino P, Cardarelli M (2015) ABCB1 and ABCB19 auxin transporters have synergistic effects on early and late *Arabidopsis* anther development. *J Integr Plant Biol*. doi:10.1111/jipb.12332
- Chang F, Wang Y, Wang S, Ma H (2011) Molecular control of microsporogenesis in *Arabidopsis*. *Curr Opin Plant Biol* 14(1):66–73
- Chaubal R, Zanella C, Trimmell MR, Fox TW, Albersten MC, Bedinger P (2000) Two male-sterile mutants of *Zea mays* (Poaceae) with an extra cell division in the anther wall. *Am J Bot* 87:1193–1201
- Chehregani A, Tanaomi N, Ranjbar M (2008) Pollen and anther development in *Onobrychis schahuensis* Borm. (Fabaceae). *Int J Bot* 4(2):241–244
- Feng X, Dickinson HG (2010) Cell-cell interactions during patterning of the *Arabidopsis* anther. *Biochem Soc Trans* 38(2):571–576
- Fisher GC (1914) Seed development in the genus *Peperomia*. *Bull Torr Bot Club* 41:221–241
- Furness CA, Rudall PJ (1998) The tapetum and systematics in monocotyledons. *Bot Rev* 64(3):201–239
- Gabarayeva N, Grigorjeva V, Rowley JR, Hemsley AR (2009a) Sporoderm development in *Trevesia burckii* (Araliaceae). I. Tetrad period: further evidence for the participation of self-assembly processes. *Rev Palaeobot Palynol* 156:211–232
- Gabarayeva N, Grigorjeva V, Rowley JR, Hemsley AR (2009b) Sporoderm development in *Trevesia burckii* (Araliaceae) II. Post-tetrad period: further evidence for the participation of self-assembly processes. *Rev Palaeobot Palynol* 156:233–247
- Heslop-Harrison J (1971) Wall pattern formation in angiosperm microsporogenesis. *Symp Soc Exp Biol* 25:277–300
- Huysmans S, El-Ghazaly G, Smets E (1998) Orbicules in Angiosperms: morphology, function, distribution, and relation with Tapetum Types. *Bot Rev* 64(3):240–272
- Igersheim A, Cichocki O (1996) A simple method for microtome sectioning of prehistoric charcoal specimens, embedded in 2-hydroxyethyl methacrylate (HEMA). *Rev Palaeobot Palynol* 92: 389–393
- Jeong BK (2005) Fine structural study of pollen wall development at late stage of microsporogenesis in *Panax ginseng*. *Kor J Electron Microsc* 35:1–10
- Julian C, Rodrigo J, Herrero M (2011) Stamen development and winter dormancy in apricot (*Prunus armeniaca*). *Ann Bot* 108:617–625
- Kelliher T, Egger RL, Zhang H, Walbot V (2014) Unresolved issues in pre-meiotic anther development. *Front Plant Sci* 21:347–355
- Kim MJ, Kim IS (1995) Microsporogenesis of *Hibiscus syriacus* L. and its sporoderm differentiation. *J Plant Biol* 38(1):95–105
- Kim YS, Lee HS, Lee MH, Yoo OJ, Liu JR (1998) A MADS Box gene Homologous to AG is expressed in seedlings as well as in flower of ginseng. *Plant Cell Physiol* 39(8):836–845
- Kim YJ, Jeon JN, Jang MG, Oh JY, Kwon WS, Jung SK, Yang DC (2014) Ginsenoside profiles and related gene expression during foliation in *Panax ginseng* Meyer. *J Ginseng Res* 38(1):66–72
- Koltunow AM, Soltys K, Nito N, McClure S (1995) Anther, ovule, seed, and nucellar embryo development in *Citrus sinensis* cv. Valencia. *Can J Bot* 73(10):1567–1582
- Kreunen SS, Osborn JM (1999) Pollen and anther development in *Nelumbo* (Nelumbonaceae). *Am J Bot* 86(12):1662–1676
- Lee OR, Sathiyaraj G, Kim YJ, In JG, Kwon WS, Kim JH, Yang DC (2011) Defense genes induced by pathogens and abiotic stresses in *Panax ginseng* C.A. Meyer. *J Ginseng Res* 35(1):21–30
- Li H, Zhang D (2010) Biosynthesis of anther cuticle and pollen exine in rice. *Plant Signal Behav* 5(9):1121–1123
- Li N, Zhang DS, Liu HS, Yin CS, Li XX, Liang WQ, Yuan Z, Xu B, Chu HW, Wang J, Wen TQ, Huang H, Luo D, Ma H, Zhang DB (2006) The rice tapetum degeneration retardation gene is required for tapetum degradation and anther development. *Plant Cell* 18(11):2999–3014
- Li H, Pinot F, Sauveplane V, Werck-Reichhart D, Diehl P, Schreiber L, Franke R, Zhang P, Chen L, Gao Y, Liang W, Zhang D (2010) Cytochrome P450 family member CYP704B2 catalyzes the {omega-ga}-hydroxylation of fatty acids and is required for anther cutin biosynthesis and pollen exine formation in rice. *Plant Cell* 22(1): 173–190
- Liu L-D, Wang Z-L, Guo-Wei T, Shen J-H (1998) Megasporogenesis, microsporogenesis and development of gametophytes in *Eleutherococcus senticosus* (Araliaceae). *Acta Phyto Sin* 36(4): 289–297
- Meloche CG, Diggle PK (2003) The pattern of carbon allocation supporting growth of preformed shoot primordia in *Acomastylis rossii* (Rosaceae). *Am J Bot* 90:1313–1320
- Mitsuda N, Seki M, Shinozaki K, Ohme-Takagi M (2005) The NAC Transcription Factors NST1 and NST2 of *Arabidopsis* regulate secondary wall thickenings and are required for anther dehiscence. *Plant Cell* 17(11):2993–3006
- Morant M, Jorgensen K, Schaller H, Pinot F, Moller BL, Werck-Reichhart D, Bak S (2007) CYP703 Is an ancient cytochrome P450 in land plants catalyzing in-chain hydroxylation of lauric acid to provide building blocks for sporopollenin synthesis in pollen. *Plant Cell* 19(5):1473–1487
- Nakamura AT, Longhi-Wagner HM, Scatena VL (2010) Anther and pollen development in some species of Poaceae (Poales). *Braz J Biol* 70:351–360
- Nuraliev MS, Oskolski AA, Sokoloff DD, Remizowa MV (2010) Flowers of Araliaceae: structural diversity, developmental and evolutionary aspects. *Plant Div Evol* 128:247–268
- Oh JY, Kim YJ, Jang MG, Joo SD, Kwon WS, Kim SY, Jung SK, Yang DC (2014) Investigation of ginsenosides in different tissues after elicitor treatment in *Panax ginseng*. *J Ginseng Res* 38(4):270–277
- Pandey AK, Dwivedi MD, Mathur RR (2014) Embryology of Cucurbitaceae and circumscription of Cucurbitales: a review. *Int J Plant Rep Biol* 6:75–98
- Parish RW, Li SF (2010) Death of a tapetum: a programme of developmental altruism. *Plant Sci* 178:73–89
- Quilichini TD, Douglas CJ, Samuels AL (2014) New views of tapetum ultrastructure and pollen exine development in *Arabidopsis thaliana*. *Ann Bot* 114(6):1189–1201
- Racich JL, Koutsky JA (1976) Nodular structure in epoxy resins. *J Appl Polym Sci* 20(8):2111–2129
- Raghavan V (1988) Anther and pollen development in rice (*Oryza sativa*). *Am J Bot* 75(2):183–196
- Reunov AA, Reunova GD, Alexandrova YN, Muzarok TI, Zhuravlev YN (2008) The pollen metamorphosis phenomenon in *Panax ginseng*, *Aralia elata* and *Oplopanax elatus*; an addition to discussion concerning the *Panax* affinity in Araliaceae. *Zygote* 17(1):1–17
- Reunova GD, Reunov AA, Aleksandrova YN, Muzarok TI, Zhuravlev YN (2007) Pollen heteromorphism in *Panax ginseng* C. A. Meyer (Araliaceae) anthers. *Dokl Biol Sci* 412:76–78
- Sajo MG, Furness CA, Prychid CJ, Rudall PJ (2005) Microsporogenesis and anther development in Bromeliaceae. *Grana* 44:65–74
- Sanders PM, Bui AQ, Weterings K, McIntire KN, Hsu YC, Lee PY, Truong MT, Beals TP, Goldberg RB (1999) Anther developmental

- defects in *Arabidopsis thaliana* male-sterile mutants. *Sex Plant Reprod* 11:297–322
- Sawhney VK, Bhadula S (2011) Microsporogenesis in the normal and male-sterile stamenless-2 mutant of tomato (*Lycopersicon esculentum*). *Can J Bot* 66:2013–2021
- Shi J, Tan H, Yu XH, Liu Y, Liang W, Ranathunge K, Franke RB, Schreiber L, Wang Y, Kai G, Shanklin J, Ma H, Zhang D (2011) Defective pollen wall of required for anther and microspore development in rice and encodes a fatty acyl carrier protein reductase. *Plant Cell* 23(6):2225–2246
- Thompson GA (1987) Botanical characteristics of ginseng. In *Herbs, Spices, and Medicinal Plants: Recent Advances in Botany, Horticulture, and Pharmacology*, Edited by: Craker LE, Simon JE Vol. 2
- Tseng CC, Shoup JR, Chuang TI, Hsieh WC (1983) Pollen morphology of *Acanthopanax* (Araliaceae). *Grana* 22:11–17
- Wen J, Nowicke JW (1999) Pollen ultrastructure of *Panax* (The ginseng genus, Araliaceae), an eastern Asian and eastern north American disjunct genus. *Am J Bot* 86(11):1624–1636
- Wilson ZA, Zhang DB (2009) From *Arabidopsis* to rice: pathways in pollen development. *J Exp Bot* 60(5):1479–1492
- Wu SS, Platt KA, Ratnayake C, Wang TW, Ting JT, Huang AH (1997) Isolation and characterization of neutral-lipid-containing organelles and globuli-filled plastids from *Brassica napus* tapetum. *Proc Natl Acad Sci U S A* 94(23):12711–12716
- Yang C, Vizcay-Barrena G, Conner K, Wilson ZA (2007) MALE STERILITY1 is required for tapetal development and pollen wall biosynthesis. *Plant Cell* 19(11):3530–3548
- Yang X, Wu D, Shi J, He Y, Pinot F, Grausem B, Yin C, Zhu L, Chen M, Luo Z, Liang W, Zhang D (2014) Rice CYP703A3, a cytochrome P450 hydroxylase, is essential for development of anther cuticle and pollen exine. *J Integr Plant Biol* 56(10):979–994
- Yeung EC, Oinam GS, Yeung SS, Harry I (2011) Anther pollen and tapetum development in safflower, *Carthamus tinctorius* L. *Sex Plant Reprod* 24(4):307–317
- Zhang D, Wilson ZA (2009) Stamen specification and anther development in rice. *Chin Sci Bull* 54(14):2342–2353
- Zhang D, Yang L (2014) Specification of tapetum and microsporocyte cells within the anther. *Curr Opin Plant Biol* 17:49–55
- Zhang D, Yuan Z (2014) Molecular control of grass inflorescence development. *Annu Rev Plant Biol* 65:553–578
- Zhang C, Guinel FC, Moffatt BA (2002) A comparative ultrastructural study of pollen development in *Arabidopsis thaliana* ecotype Columbia and male-sterile mutant *apt1-3*. *Protoplasma* 219(1–2):59–71
- Zhang Z, Kang X, Wang S, Li D, Chen H (2009) Pollen development and multi-nucleate microspores of *Populus bolleana* Lauche. *For Stud China* 10:107–111
- Zhang D, Luo X, Zhu L (2011) Cytological analysis and genetic control of rice anther development. *J Genet Genomics* 38(9):379–390
- Zhang Y, Liang W, Shi J, Xu J, Zhang D (2013) MYB56 encoding a R2R3 MYB transcription factor regulates seed size in *Arabidopsis thaliana*. *J Integr Plant Biol* 55(11):1166–1178
- Zhao D (2009) Control of anther cell differentiation: a teamwork of receptor-like kinases. *Sex Plant Reprod* 22(4):221–228